Journal of Power Sources 185 (2008) 603–608

Contents lists available at ScienceDirect

Journal of Power Sources

journal homepage: www.elsevier.com/locate/jpowsour

The methanol adsorption behavior on platinum/poly(2,5-dimethoxyaniline) composites for application in methanol sensing

Tang-Kuei Chang[a], Chia-Chin Chang[b], Ten-Chin Wen[a,*]

[a] Department of Chemical Engineering, National Cheng Kung University, Tainan 70101, Taiwan
[b] Department of Environment and Energy, National University of Tainan, Tainan 70101, Taiwan

ARTICLE INFO

Article history:
Received 25 July 2008
Received in revised form 8 September 2008
Accepted 8 September 2008
Available online 19 September 2008

Keywords:
Direct methanol fuel cells
Methanol adsorption
Methanol sensing
Platinum/poly(2,5-dimethoxyaniline) composites

ABSTRACT

The behavior of methanol adsorption on platinum/poly(2,5-dimethoxyaniline) (Pt/PDMA) composite is investigated using UV–vis spectroscopy (UV–vis) and open circuit potential (OCP). The results of scanning electron microscopy and energy dispersive spectroscopy are used to verify the uniform dispersion of Pt in PDMA. The Fourier transform infrared spectra and OCP results revealed that Pt particles interact with PDMA through the electron-rich nitrogen sites, influencing the oxidation state of PDMA. A model is proposed for the methanol adsorption on Pt particles which changes the interaction between Pt and PDMA. With the proposed model, methanol concentration can be discerned using potentiometric measurements. The results of this study can be applied to methanol sensors for direct methanol fuel cells.

1. Introduction

Conducting polymer–metal composites have attracted interest due to their properties, which are different from those of pure conducting polymers and metals [1,2]. They can be used as a suitable catalyst for direct methanol fuel cells (DMFCs) [3–6] or as sensing materials for chemical sensors [7–10]. In DMFCs, the homogenous dispersion of metal particles inside conducting polymer can decrease the amount of noble metal required. The composites also exhibit better catalytic performance than that of the bulk-form of metal electrodes for the oxidation of methanol. As chemical sensors, conducting polymer–metal composites are highly sensitive and show a fairly good response due to their unique surface activities. A large number of studies on the electrocatalytic properties of Pt metal and its alloys incorporated into polymeric matrices have been published during the last 5 years [11–17] but very few reports have been published on the composite formation of platinum/poly(2,5-dimethoxyaniline) (Pt/PDMA).

Poly(2,5-dimethoxyaniline) (PDMA) is a PANI derivative which contains the methoxy ($-OCH_3$) groups substituted at o- and m-positions with respect to nitrogen atoms. It can be easily polymerized and switched from leucoemeraldine or emeraldine to be more oxidized than PANI at a low potential [18]. The electron donating methoxy groups in the aromatic ring can provide a suitable environment for reducing metal ions (e.g. Pt^{4+}) through the amine groups in PDMA [19]. We thus investigated the possibility of using Pt deposited in PDMA. The introduction of Pt can strongly influence the electronic and chemical properties of the conducting polymer because of the close contact between the conducting polymer and Pt [20,21]. The adsorption of small organic molecules like methanol on the Pt surface, which dehydrogenates rapidly at 140 K [22], might affect the interaction of the conducting polymer and Pt. Accordingly, the state of the conducting polymer could be changed for discerning organic molecules.

The aim of this work was to study the methanol adsorption behavior of pure PDMA film and Pt/PDMA composite electrodes in aqueous acid solutions. The mechanism of methanol adsorption on Pt/PDMA is proposed. Scanning electron microscopy (SEM), Fourier transform infrared spectra (FTIR), UV–vis spectrophotometry (UV–vis), and the open circuit potential (OCP) test were used in the investigation.

2. Experimental

2.1. Chemicals and solutions

Reagent grade 2,5-dimethoxyaniline (DMA, Fluka), hydrochloric acid (Riedel-de Haën), sulfuric acid (Merck), and methanol (Merck) were used without any further treatment. H_2PtCl_6 was obtained from Alfa Aesar.

* Corresponding author. Tel.: +886 6 2385487; fax: +886 6 2344496.
E-mail address: tcwen@mail.ncku.edu.tw (T.-C. Wen).

0378-7753/$ – see front matter © 2008 Elsevier B.V. All rights reserved.
doi:10.1016/j.jpowsour.2008.09.033

2.2. Apparatus

Electrochemical synthesis and open circuit potential measurements were performed with PGSTAT 30, Autolab (Eco. Chemie B.V., The Netherlands). A three-electrode cell assembly was used with Ag/AgCl (in 3 M KCl), Pt wire, and an ITO coated glass plate (1 cm^2 area) as the reference, counter, and working electrodes, respectively. A Luggin capillary, whose tip was set at a distance of about 1 mm from the surface of the working electrode, was used to minimize errors due to *iR* drop in the electrolytes. The potentials reported here are with respect to Ag/AgCl as the reference electrode. All experiments were carried out at room temperature ($25 \pm 1\,^{\circ}C$). The surface morphologies of PDMA and Pt/PDMA were observed with SEM (JEOL JSM-6700F) and analyzed by an energy dispersive spectrometer (EDS) (OXFORD INCA400). The FTIR spectra of PDMA and Pt/PDMA in KBr pellets were recorded using a Nicolet Nexus 470 FTIR spectrophotometer. A Shimadzu MultiSpec-1500 UV–vis spectrophotometer was used to record the *in situ* UV–vis spectra using the time course mode. UV–vis spectroelectrochemical experiments were done in a quartz cuvette using an electrochemical cell with an optically transparent working electrode, a Pt wire as the counter electrode, and Ag/AgCl as the reference electrode.

2.3. Preparation of PDMA and Pt/PDMA composite films

PDMA film was prepared using electrochemical polymerization (at a constant potential of 0.8 V vs. Ag/AgCl) in 1 M HCl with 50 mM DMA. The deposited films were then rinsed in double distilled water to remove oligomers and dried for further deposition of Pt particles. Pt particles were electrodeposited into PDMA at −0.2 V in 0.01 M HCl and 0.1 M KCl with 5 mM $H_2PtCl_6{\cdot}H_2O$. The deposition amount was controlled by a charge of 0.2 C. Prior to the experiment, the electrode was soaked in the above solution for 3 min. After Pt deposition, the electrode was rinsed with double distilled water and then dried.

3. Results and discussion

3.1. Morphology of PDMA and the Pt/PDMA composite

SEM images of PDMA and the Pt/PDMA composite are shown in Fig. 1a and b, respectively. In Fig. 1a, the PDMA growth from acidic media resulted in a porous-structure with a high surface area polymer film. Fig. 1b shows the morphology of the Pt/PDMA composite, which was prepared by the potentiostatical electrodeposition of Pt on PDMA/ITO. The pores of the polymer are visible, with Pt particles appearing in the voids. The particle size was between 100 and 200 nm. The Pt particles were uniformly dispersed on the PDMA surface. The EDS results prove the existence of Pt in the composite as shown in Fig. 1c.

3.2. FTIR spectroscopy of PDMA and the Pt/PDMA composite

FTIR spectra of PDMA and the Pt/PDMA composites are shown in Fig. 2. Both had similar characteristic peaks. The broad peak around 3000–3500 cm^{-1} is O–H stretching [23]. Bands that are characteristic of C–N stretching are in the range of 1250–1300 cm^{-1} [24]. The peak at 830 cm^{-1} corresponds to C–H out-of-plane vibrations of the 1,4-disubstituted benzene ring [25]. Bands around 1500 and 1600 cm^{-1} can be assigned to the non-symmetric C_6 ring vibrational bands. The higher frequency vibration represents the quininoid ring and the lower one represents the benzenoid ring. These two bands clearly show that these polymers are composed of amine and imine units. The relative intensity of these two bands can be taken as the extent of oxidation states in these materials

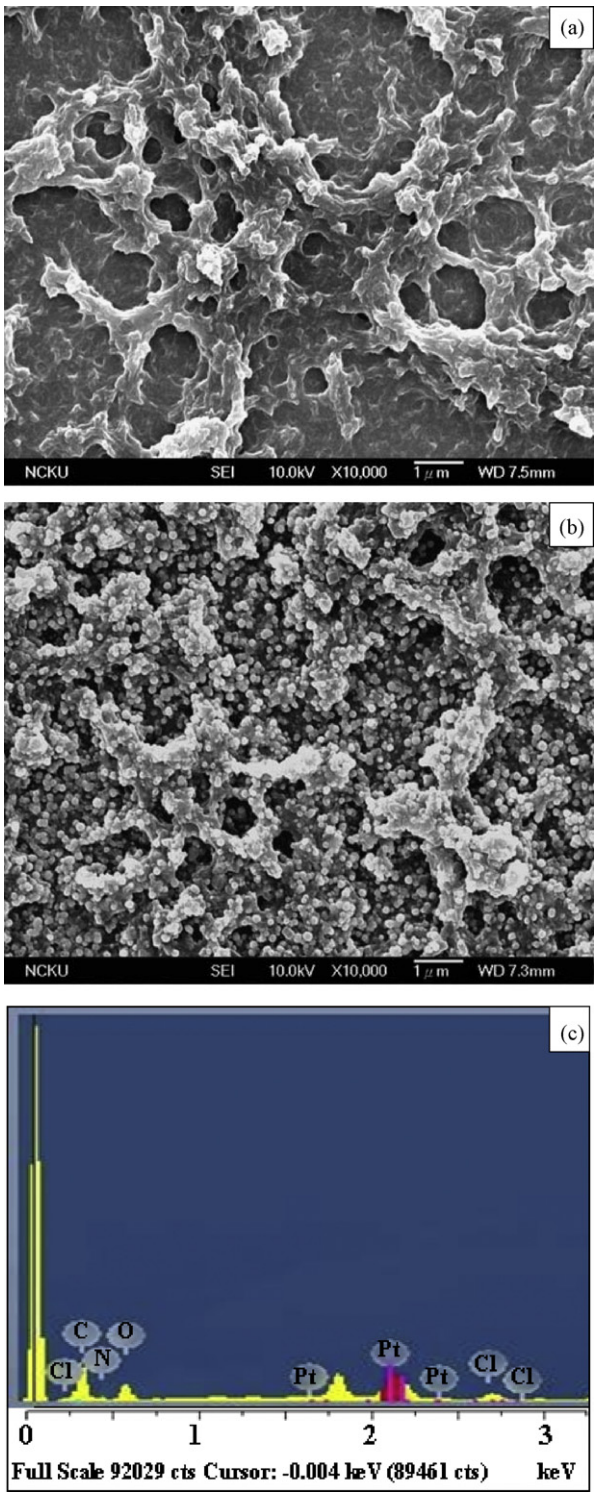

Fig. 1. (a) SEM micrograph of PDMA, (b) SEM micrograph of Pt/PDMA and (c) EDS plot.

[24]. The two characteristic peak assignments of Fig. 2 are summarized in Table 1. The ratio *R* (imine vs. amine units) is an estimation of the oxidation state of the polymer [26]. The ratio *R* of Pt/PDMA is higher than that of PDMA, which indicates a relatively larger number of oxidized units (in imine form). The oxidation state of PDMA is increased by Pt because Pt deposited on PDMA may interact with nitrogen and hydrogen (N–H bonds). As shown in Scheme 1, Pt par-

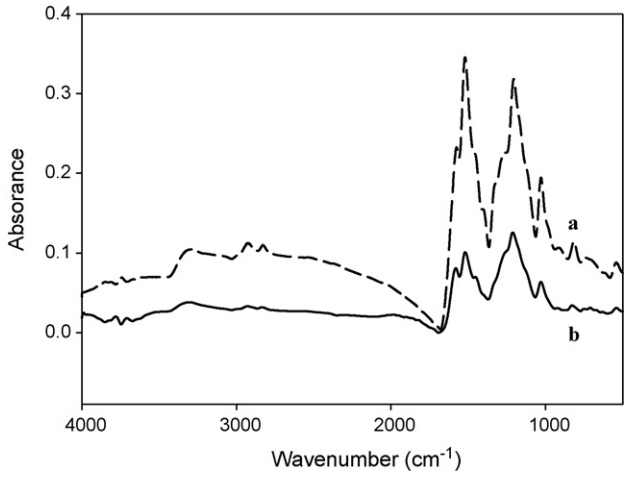

Fig. 2. FTIR spectra of PDMA (- - -) and Pt/PDMA (—).

ticles were reduced at −0.2 V. The state of PDMA is known as the completely reduced leucoemeraldine state. $PtCl_6^{2-}$ is then reduced by PDMA at amine sites producing a larger concentration of the imine group in the polymer. The intrinsic state of PDMA is changed to produce a more oxidized polymer.

3.3. Open circuit potential of PDMA and the Pt/PDMA composite

To investigate the effect of Pt on the intrinsic state of PDMA, OCP experiments were performed on PDMA and Pt/PDMA electrodes. Fig. 3a shows the time dependence of OCP for PDMA and Pt/PDMA in 0.5 M H_2SO_4 at room temperature. The value of OCP is higher for Pt/PDMA than it is for PDMA, suggesting that the interaction between Pt particles and PDMA directly affects the oxidation state of PDMA. These results are in good agreement with the FTIR data. To understand the electronic state of PDMA and Pt/PDMA in acid solution, cyclic voltammograms of PDMA were recorded in 0.5 M H_2SO_4; they are shown in Fig. 3b. The two redox peaks A/A′ and B/B′ are attributed to leucoemeraldine to emeraldine and emeraldine to pernigraniline transitions, respectively. The stable states of Pt/PDMA and PDMA are pernigraniline and emeraldine, respectively.

3.4. UV–vis spectrophotometric and potentiometric response characteristics of Pt/PDMA composites for methanol adsorption

Pt is a common catalyst in methanol (CH_3OH) dehydrogenation [22,27]. The interaction between Pt and methanol might affect the redox state of PDMA. A preliminary test was performed using UV–vis spectroscopy. Fig. 4 shows the UV–vis spectra of PDMA and Pt/PDMA film on the ITO electrode at various concentrations of CH_3OH in 0.5 M H_2SO_4. Fig. 4a shows that the peaks at 350, 450, and 770 nm, can be attributed to the π–π* transition of the aromatic benzene ring (leucoemeraldine), polaron–π, π–π (emeraldine), and polaron–π* transitions (pernigraniline), respectively. These results are similar to those published in previous reports [26,28]. The spectra of PDMA (Fig. 4a) are almost the same at methanol concentrations from 0 to 3 M, implying that there is no interaction

Table 1
R ratio of PDMA and Pt/PDMA.

Sample	Imine	Amine	*R* = imine/amine (%)
PDMA	0.4	0.6	65.71
Pt/PDMA	0.44	0.56	80.81

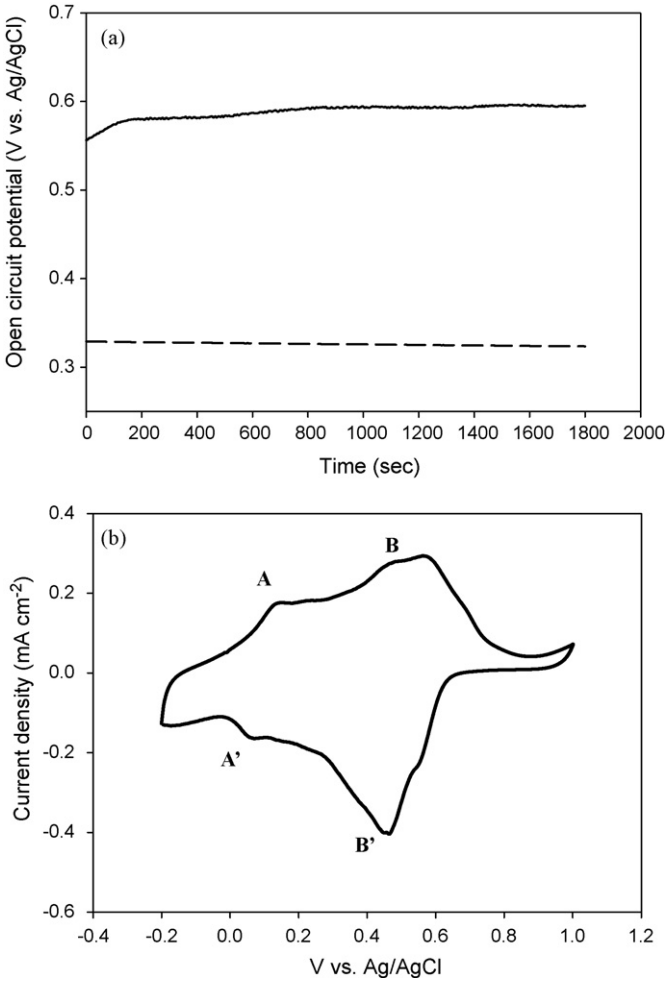

Fig. 3. (a) Open circuit potential for PDMA (- - -) and Pt/PDMA (—) in 0.5 M H_2SO_4. (b) Cyclic voltammograms of PDMA in 0.5 M H_2SO_4 at a scan rate = 10 mV s^{-1}.

between methanol and PDMA. In contrast to PDMA, the spectral changes of Pt/PDMA at various concentrations of methanol are clear, as shown in Fig. 4b. Note that the pernigraniline form (770 nm) decreases until it disappears and the emeraldine form (450 nm) increases with increasing methanol concentration.

Interestingly, the interaction between Pt and PDMA is changed by absorbed methanol, which shows the catalytic activity of Pt on methanol dehydrogenation. The methanol adsorbed on the Pt surface can influence the PDMA transitions from the oxidation state (pernigraniline) to the reduction state (emeraldine). This can be observed from the difference of OCP data using $\Delta E = E_p - E_m$, where E_p and E_m represent the OCP data for Pt/PDMA in 0.5 M H_2SO_4 without and with methanol, respectively. Fig. 5 shows the dependence of ΔE on the concentration of CH_3OH for PDMA and the Pt/PDMA composite electrodes. For the PDMA electrode, ΔE seems to be invariant with methanol concentration. For the Pt/PDMA electrode, ΔE linearly increases with increasing CH_3OH concentration. The slope of the Pt/PDMA electrode was calculated to be 41.45 mV per log[CH_3OH] ($r^2 = 0.9911$). The linear increase with methanol makes Pt/PDMA a potential material for methanol sensing. In this study, the methanol concentration was limited to 3 M because the methanol feed concentration range was usually lower than 5 M [29–32]. The reason for low methanol concentration range is that the cell performance is dramatically reduced at the high methanol concentration due to the problem of methanol crossover.

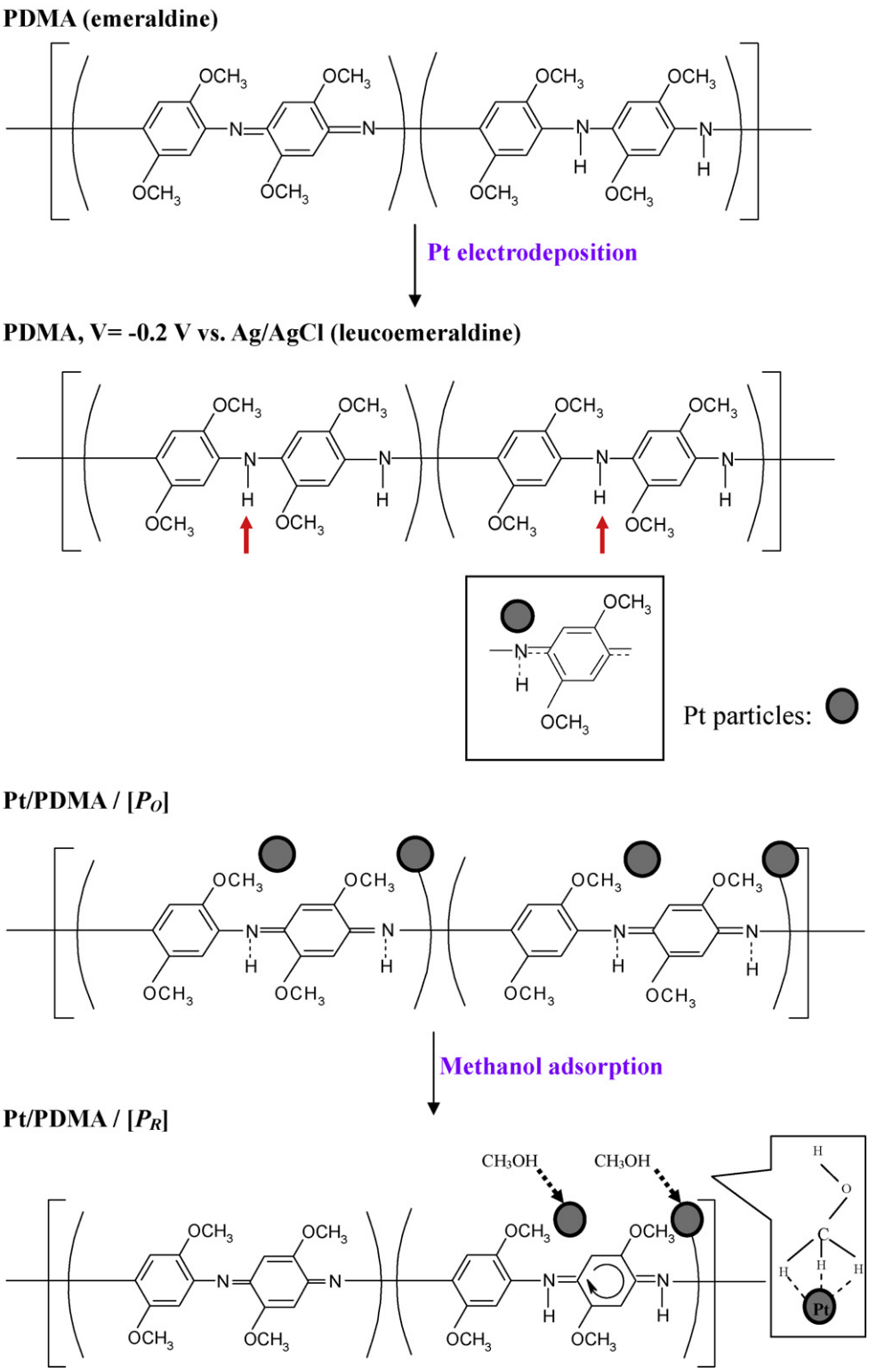

Scheme 1. Schematic representation of the interaction of Pt particles on PDMA during (1) Pt electrodeposition and (2) methanol adsorption.

3.5. The mechanism of methanol adsorption on Pt/PDMA

Based on the above results and discussion, the following mechanism for the dissociative adsorption–dehydrogenation of methanol is assumed to be established at the Pt/PDMA electrode:

$$CH_3OH + Pt \Leftrightarrow (CH_3OH)_{ads} + Pt \quad (1)$$

$$(CH_3OH)_{ads}Pt \rightarrow (CH_{3-x}OH)_{ads}Pt + xH^+ + xe^- \quad (2)$$

The potential (E_m) of reaction (2) can be expressed by the Nernst equation as

$$E_m = E^{0'}_{[(CH_{3-x}OH)_{ads}Pt][H^+]^x/[(CH_3OH)_{ads}Pt]} + \frac{RT}{xF}\ln\frac{[(CH_{3-x}OH)_{ads}Pt][H^+]^x}{[(CH_3OH)_{ads}Pt]} \quad (3)$$

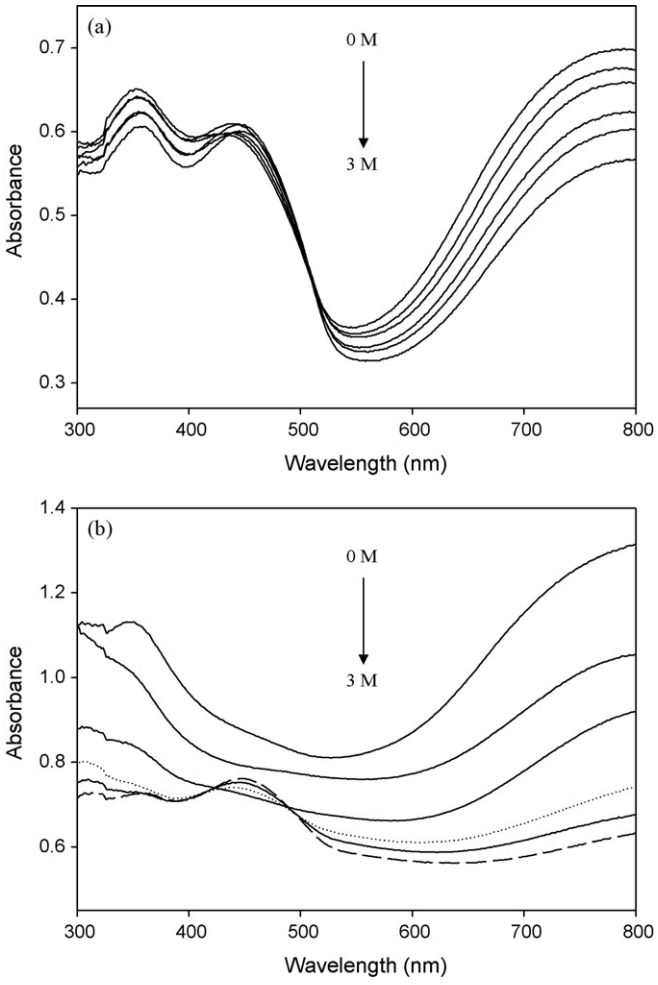

Fig. 4. UV–vis spectrum of (a) PDMA and (b) Pt/PDMA at various concentrations of CH_3OH in 0.5 M H_2SO_4: 0, 0.1, 0.5, 1, 2, and 3 M.

where $E^{0'}$ is the standard electrode potential. From reaction (1), the adsorption constant of methanol molecules is defined as

$$K_A = \frac{[(CH_3OH)_{ads}Pt]}{[CH_3OH]} \tag{4}$$

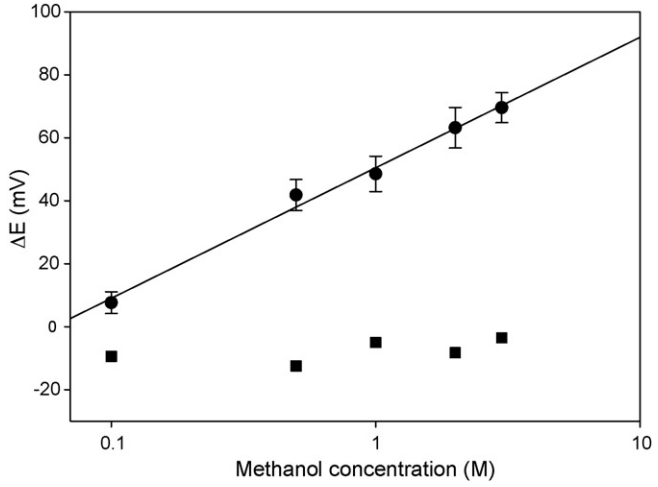

Fig. 5. The variation of ΔE for PDMA (■) and Pt/PDMA (●) at various concentrations of CH_3OH in 0.5 M H_2SO_4: 0.1, 0.5, 1, 2, and 3 M.

Substituting Eq. (4) into Eq. (3) gives

$$E_m = E^{0'}_{[(CH_{3-x}OH)_{ads}Pt][H^+]^x/[(CH_3OH)_{ads}Pt]} + \frac{RT}{xF}\ln\frac{[(CH_{3-x}OH)_{ads}Pt][H^+]^x}{K_A[CH_3OH]} \tag{5}$$

The interaction between Pt and methanol affects the state of PDMA, which is briefly sketched in Scheme 1. The oxidation state of PDMA is increased due to the deposition of Pt on the PDMA surface. The interaction between Pt and PDMA is changed by the adsorption of methanol on Pt, decreasing the oxidation state of PDMA. The redox chemistry of PDMA can be written as

$$P_O + xH^+ \Leftrightarrow P_OH_x^{x+} \tag{6}$$

$$P_OH_x^{x+} + xe^- \Leftrightarrow P_R \tag{7}$$

where P_O and P_R represent the oxidation state and reduction state of PDMA, respectively.

From reaction (6), the dissociation constant of PDMA is given by

$$K_a = \frac{[P_O][H^+]^x}{[P_OH_x^{x+}]} \tag{8}$$

The potential (E_p) of reaction (7) can be expressed by the Nernst equation as

$$E_p = E^{0'}_{[P_OH_x^{x+}/P_R]} + \frac{RT}{xF}\ln\frac{[P_OH_x^{x+}]}{[P_R]} \tag{9}$$

The overall reaction (combining reactions (6) and (7)) becomes

$$P_O + xH^+ + xe^- \Leftrightarrow P_R \tag{10}$$

When $[P_OH_x^{x+}]$ from Eq. (8) is substituted into Eq. (9), the Nernst equation for the net reaction becomes

$$E_p = E^{0'}_{[P_OH_x^{x+}]/[P_R]} + \frac{RT}{xF}\ln\frac{[P_O][H^+]^x}{K_a[P_R]} \tag{11}$$

Subtracting Eq. (11) from Eq. (5) and defining $\Delta E = E_p - E_m$ gives

$$\Delta E = E^{0'}_{[P_OH_x^{x+}]/[P_R]} - E^{0'}_{[(CH_{3-x}OH)_{ads}Pt][H^+]^x/[(CH_3OH)_{ads}Pt]} + 2.303\frac{RT}{xF}\left(\log\frac{K_A}{K_a} + \log\frac{[P_O]}{[P_R]} + \log\frac{1}{[(CH_{3-x}OH)_{ads}Pt]} + \log[CH_3OH]\right) \tag{12}$$

A plot of ΔE versus $\log[CH_3OH]$ yields a straight line with a slope of $2.303RT/xF$. It is clear that x represents the electron transfer or the proton relaxation number from Eqs. (6) and (7). The value of x for Pt/PDMA is 1.4; x is about 1 for pure Pt catalyst [33]. Because the value of x (1.4) is greater than 1, the dissociative adsorption–dehydrogenation of methanol on Pt/PDMA is more efficient than that on pure Pt. This behavior is useful for methanol sensors in DMFCs.

4. Conclusion

A composite of PDMA with Pt nanoparticles (Pt/PDMA) was successfully prepared to study methanol adsorption behavior. The oxidation state of Pt/PDMA composite depends on the methanol adsorption, as confirmed by UV–vis spectrophotometric and potentiometric measurements. The linear response of ΔE for different concentrations (0–3 M) of methanol absorbed on the Pt/PDMA electrode can be effectively used as a methanol sensor in DMFCs.

Acknowledgements

The financial support of this work by the National Science Council of Taiwan under grants NSC-95-2211-E-006-409-MY3 and NSC-96-221-E-006-059 is gratefully acknowledged.

References

[1] R. Gangopadhyay, A. De, Chem. Mater. 12 (2000) 608.
[2] D.W. Hatchett, M. Josowicz, Chem. Rev. 108 (2008) 746.
[3] B. Rajesh, K.R. Thampi, J.M. Bonard, H.J. Mathieu, N. Xanthopoulos, B. Viswanathand, Electrochem. Solid State Lett. 7 (2004) A404.
[4] L. Niu, Q. Li, F. Wei, S. Wu, P. Liu, X. Cao, J. Electroanal. Chem. 578 (2005) 331.
[5] C.W. Kuo, L.M. Huang, T.C. Wen, A. Gopalan, J. Power Sources 160 (2006) 65.
[6] V. Selvaraj, M. Alagar, I. Hamerton, J. Power Sources 160 (2006) 940.
[7] H. Zhoua, H. Chena, S. Luob, J. Chena, W. Wei, Y. Kuang, Biosens. Bioelectron. 20 (2005) 1305.
[8] A.A. Athawale, S.V. Bhagwat, P.P. Katre, Sens. Actuators B: Chem. 114 (2006) 263.
[9] S. Sharma, C. Nirkhe, S. Pethkar, A.A. Athawale, Sens. Actuators B: Chem. 85 (2002) 131.
[10] J. Mathiyarasu, S. Senthilkumar, K.L.N. Phani, V. Yegnaraman, Mater. Lett. 62 (2008) 571.
[11] L. Niu, Q. Li, F. Wei, X. Chen, H. Wang, Synth. Met. 139 (2003) 271.
[12] B. Rajesh, K.R. Thampia, J.M. Bonard, A.J. McEvoy, N. Xanthopoulos, H.J. Mathieu, B. Viswanathan, J. Power Sources 133 (2004) 155.
[13] F. Xie, Z. Tian, H. Meng, P.K. Shen, J. Power Sources 141 (2005) 211.
[14] G. Wu, L. Li, J.H. Li, B.Q. Xu, J. Li, J. Power Sources 155 (2006) 118.
[15] S.P. Jiang, Z. Liu, H.L. Tang, M. Panb, Electrochim. Acta 51 (2006) 5721.
[16] V. Selvaraj, M. Alagar, Electrochem. Commun. 9 (2007) 1145.
[17] L.M. Huang, W.R. Tang, T.C. Wen, J. Power Sources 164 (2007) 519.
[18] L.M. Huang, T.C. Wen, A. Gopalan, Mater. Chem. Phys. 77 (2002) 726.
[19] L.M. Huang, T.C. Wen, Mater. Sci. Eng. A: Struct. 445 (2007) 7.
[20] D.W. Hatchett, R. Wijeratne, J.M. Kinyanjui, J. Electroanal. Chem. 593 (2006) 203.
[21] J.M. Kinyanjui, N.R. Wijeratne, J. Hanks, D.W. Hatchett, Electrochim. Acta 51 (2006) 2825.
[22] B.A. Sexton, Surf. Sci. 102 (1981) 271.
[23] C.S. Wu, F.Y. Lin, C.Y. Chen, P.P. Chua, J. Power Sources 160 (2006) 1204.
[24] T.C. Wen, L.M. Huang, A. Gopalan, Synth. Met. 123 (2001) 451.
[25] M. Jayakannan, P. Anilkumar, A. Sanju, Eur. Polym. J. 42 (2006) 2623.
[26] J.M. Kinyanjui, J. Hanks, D.W. Hatchett, A. Smith, M. Josowicz, J. Electrochem. Soc. 151 (2004) D113.
[27] J. Kua, W.A. Goddard, J. Am. Chem. Soc. 121 (1999) 10928.
[28] S.K. Pillalamarri, F.D. Blum, A.T. Tokuhiro, M.F. Bertino, Chem. Mater. 17 (2005) 5941.
[29] K. Scott, W.M. Taama, J. Cruickshank, J. Power Sources 65 (1997) 159.
[30] K. Scott, W.M. Taama, P. Argyropoulos, K. Sundmacher, J. Power Sources 83 (1999) 204.
[31] S.H. Liang, C.C. Liu, C.H. Tsaia, J. Electrochem. Soc. 153 (2006) H138.
[32] H. Zhao, J. Shen, J. Zhang, H. Wang, D.P. Wilkinson, C.E. Gua, J. Power Sources 159 (2006) 626.
[33] E. Leiva, M. Giordano, J. Electrochem. Soc. 130 (1983) 1305.